Canadian Conference - Pacific Conference on Earthquake Engineering 2023
Vancouver, British Columbia
June 25th – June 30th, 2023

Initial Performance and Reliability Assessment of a Frictional GripNGrab Device during Experimental Component Testing

Kiran Rangwani[1*], Geoffrey W. Rodgers[2], Gregory MacRae[3], Shahab Ramhormozian[4], Charles Clifton[5] and Zhenduo Yan[6]

[1]PhD Student, Department of Civil and Natural Resource Engineering, University of Canterbury, Christchurch, New Zealand
[2]Professor, Department of Mechanical Engineering, University of Canterbury, Christchurch, New Zealand
[3]Professor, Department of Civil and Natural Resource Engineering, University of Canterbury, Christchurch, New Zealand
[4]Senior Lecturer, School of Future Environments, Auckland University of Technology, Auckland, New Zealand
[5]Professor, Department of Civil and Environmental Engineering, The University of Auckland, Auckland, New Zealand
[6]PhD Student, Department of Civil and Environmental Engineering, The University of Auckland, Christchurch, New Zealand
[*]gregory.macrae@canterbury.ac.nz (Corresponding Author)

ABSTRACT

The large-scale experimental component testing of a frictional "GripNGrab (GNG)" tension-only dissipation device is described. The 2.2m long device consists of a (i) ratcheting part, and (ii) sliding frictional dissipation part. When the device is subjected to shortening displacements, ratcheting occurs and the compressive force is small (less than 1kN), thereby avoiding buckling or the need to significant buckling restraint. Conversely, for elongating displacements, teeth in the ratchet engage, allowing significant tensile force to be carried. The frictional dissipators, used in a symmetric friction configuration, consisted of plates, shims, and conical spring washers (CSWs) or structural washers clamped together using high strength bolts. Slotted holes in the central friction plate allow large sliding displacements of up to 500mm. The device is subjected to various cyclic unipolar "extension and return to initial displacement" test regimes to represent the behaviour expected of such a device when installed between a foundation and the base of a rocking frame, where full post-earthquake recentring is required. A total of thirty-eight tests were conducted and parameters varied including the device initial axial tension force, the GNG ratchet pitch, frictional components, and dissipator bolting arrangement (M12 and M16 bolts, with and without the use of CSWs), and the dissipator bolt clamping force. From this range of tests, the comprehensive findings for 5 experimental tests are discussed in detail. It is shown that the ratcheting device behaved as expected, however the frictional sliding resistance force was sometimes less than 40% of the predicted design sliding forces. The average effective sliding coefficient of friction obtained from the tests was approximately 24% lower than the designed value. Potential reasons for the low frictional resistance forces are discussed. For all the test cases, the maximum compressive force obtained was less than 1 kN, as intended by design.

Keywords: GripNGrab (GNG), tension-only dissipation device, experimental component test, ratcheting, friction sliding.

1 INTRODUCTION TO ROCKING FRAME GNG

1.1 Background, Need & Scope

Standard energy dissipators placed at the base of rocking frames can lessen frame displacement demands and reduce structural and non-structural damage. However, there is a risk of buckling with standard dissipators during compressive loading and frame permanent displacements are possible if post-tensioning and gravity forces are not sufficient to overcome the compressive resistance provided by the dissipaters [1]. Furthermore, if the dissipaters can sustain residual compressive forces after re-seating of the wall, these compressive forces can partially offset the clamping effects of post-tensioning, resulting in a lower resistance to the onset of rocking during subsequent earthquakes. To solve these issues, tension-only dissipators like the Friction GripNGrab (GNG) can be used, as they dissipate energy in tension and ratchet in compression, allowing frames to fully recentre and eliminating the likelihood of buckling as there is only a small compression force. Additionally, the frictional dissipation component of the GNG allows for larger displacements without significant damage to the frame compared to yielding dissipators [2, 3]. A friction GNG is proposed to be implemented in the full-scale shake-table testing of a ROBUST building

project that includes a rocking frame (in a transverse direction) to evaluate the overall performance of the building. Before the GNG dissipator is used in the full-scale shake-table test of the Robust rocking frame building, it is important to evaluate the effectiveness of these simple, non-buckling, and low-cost GNG friction devices through experimental component testing.

This paper addresses the full-scale component experimental testing of the frictional GNG for rocking frame systems by seeking answers to the following questions:

1. How does the ratcheting GNG dissipation device behave?
2. Can such a GNG device with frictional dissipation be designed and constructed?
3. Does the device behave predictably and consistently?

2 LITERATURE REVIEW

2.1 Rocking frames

Although rocking frames can have recentring issues [4], they have gained popularity as a concept to lessen earthquake damage caused by earthquake shaking [5]. Several methods can be used to dissipate energy [4, 6, 7]). The performance of the structures is improved by incorporating various methods of energy dissipation, such as base isolation, lead dissipators by Rodgers et al. [8], buckling restrained frames (BRBs) [9], etc. However, using tension-only devices is one of the suggested methods that enables the structure to statically recenter and have the same resistance to uplift on subsequent loading cycles. The displacement requirements can be decreased by including energy dissipation in comparison to not including it [7, 10, 11]. Gravity, posttensioning, slab effects, and dissipation devices can provide restoring forces for rocking structures [7, 12, 13]. Using a tension-only device, such as the "Grip N Grab" (GNG) device, is one energy dissipation method that not only offers dissipation but also enables full self-centering and may be able to prevent the structure from experiencing excessive drifts [3, 12].

2.2 Tension only dissipation device – GNG

An energy dissipation device can reduce the displacement demand of rocking walls and building structures. However, devices that exhibit elasto-plastic hysteresis such as yielding steel undergo compression and may have problems with buckling during compression loading, especially under the combination of in-plane, and out-of-plane, action as observed by Gultom and Ma [1]. Furthermore, if the dissipation device strength is too high, the structure may not re-seat after a major earthquake event [4].

A "tension only device," also known as the "GripNGrab (GNG)" energy dissipation device, which is based on the cable tie concept, has been developed to resolve these problems. This device ensures the static self-centering of rocking structures and eliminates the risk of buckling because there is little compression force. The total deformation capacity of these tension-only dissipaters is determined by the number of cycles and amplitude of tension movements during frame uplift. The GNG device consists of two components i.e., ratcheting component and dissipation component where the energy is dissipated under tension and ratchet in compression [4, 10]). It has been used in a tension-only yielding braced system focusing on out-of-plumb effects by Rad et al. [14, 15] and it shows promise for rocking structures, where an overly stiff device does not lead to excessive displacements in the out-of-plane direction. Furthermore, experimental testing of the GNG component which uses a yielding dissipator, conducted by Cook et al. [2, 3], has shown a good match with analysis results using a GNG hysteresis model.

Although the ratcheting GNG engagement concept can be used with any energy dissipation mechanism, the energy dissipator that has been used in past is only yielding dissipators. Moreover, the displacement capacity of yielding dissipators (as a percentage of their length) is rather small [2, 3, 14]. A frictional GNG can achieve large displacements without causing significant damage. Livia & Yoo [16] did a preliminary study on frictional GNG with a rocking frame, using a small-scale conceptual rocking model with frictional GNG to demonstrate this novel idea. A novel frictional GNG has been designed in this research with the potential to provide large displacements without incurring significant damage.

2.3 Frictional GNG performance when used with a rocking frame.

Figure 1 illustrates the friction GNG, which consists of two primary components: the ratcheting component and the dissipation (in this research, frictional) component. Energy is absorbed when the device is under tension by sliding within the frictional component. When the device is loaded in the compression direction, almost no force is carried, so the device does not buckle, but displacement occurs in the ratcheting component. This tension only direction of ratchet teeth engagement helps eliminate residual compressive forces is described in detail in Rangwani et al. [13] and is also shown in **Figure 1(b).** The ratcheting during the shortening of the device as the frame base returns to the foundation allows recentring. When the teeth engage during tension-loading, energy dissipation occurs in the sliding frictional component. It is worth noting that the ratcheting action essentially accumulates inelastic displacement across successive response cycles, so the device needs to be designed with significant displacement capacity within both the rack (where ratcheting occurs) and within the sliding frictional dissipater.

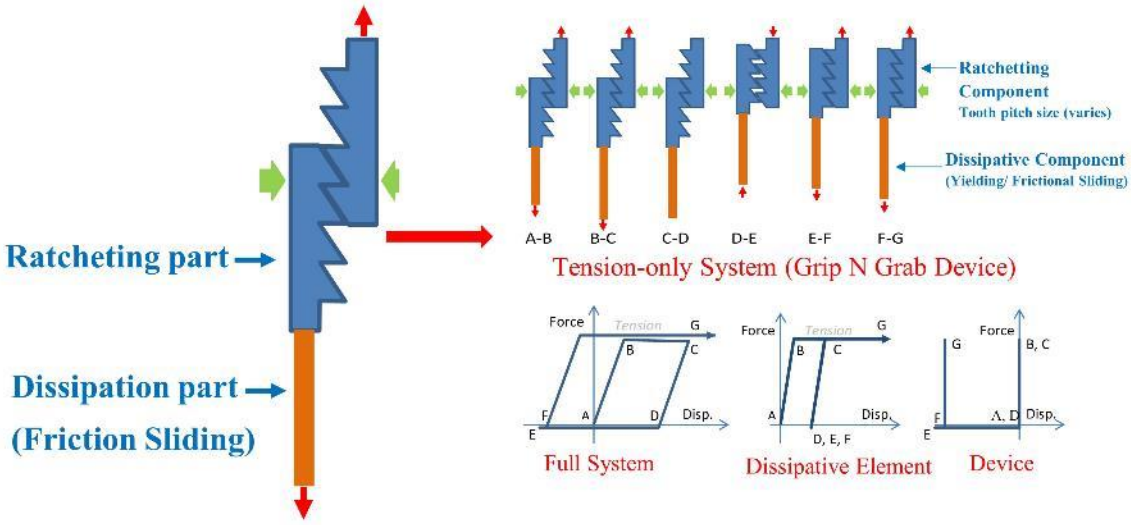

(a) Schematic *(b) Behaviour [5]*

Figure 1 GNG Frictional Device

In order to investigate the overall performance of the building, the frictional GNG is planned to be used in a ROBUST building project that comprises a 3-storey steel rocking frame that is 9.0 m tall and 4.75 m wide in the transverse direction. **Figure 2(a)** depicts the ROBUST building with a V-braced rocking frame in the transverse direction, and **Figure 2(b)** depicts the friction GNG installed at the corner bases of the rocking frame. Experimental component testing of GNG friction device was done in order to evaluate their performance prior to the GNG dissipator being implemented in the ROBUST rocking frame building. The current paper's framework is defined by the test plan, device friction behaviour, and test results, which will be discussed in more detail in the following sections.

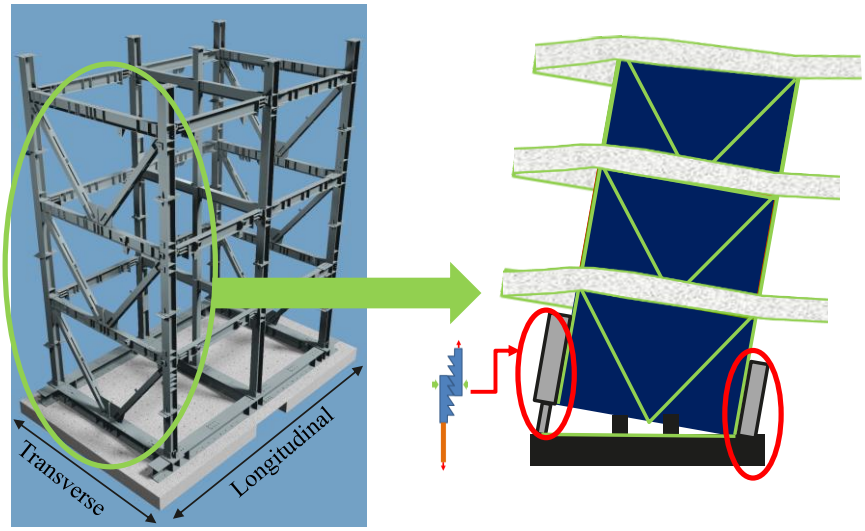

(a) ROBUST Building [17] *(b) Rocking Frame with GNG Device*

Figure 2: ROBUST test programme at International Joint Research laboratory of Earthquake Engineering (ILEE) [18]

3 METHODOLOGY

3.1 Frictional GNG device behaviour

The frictional GNG device is a type of energy dissipator that consists of (i) a ratcheting part, which carries large forces in tension but only minimal forces in compression as it ratchets, and (ii) a friction sliding dissipation part, which dissipates energy in friction (**Figures 1 and 3(a)).**

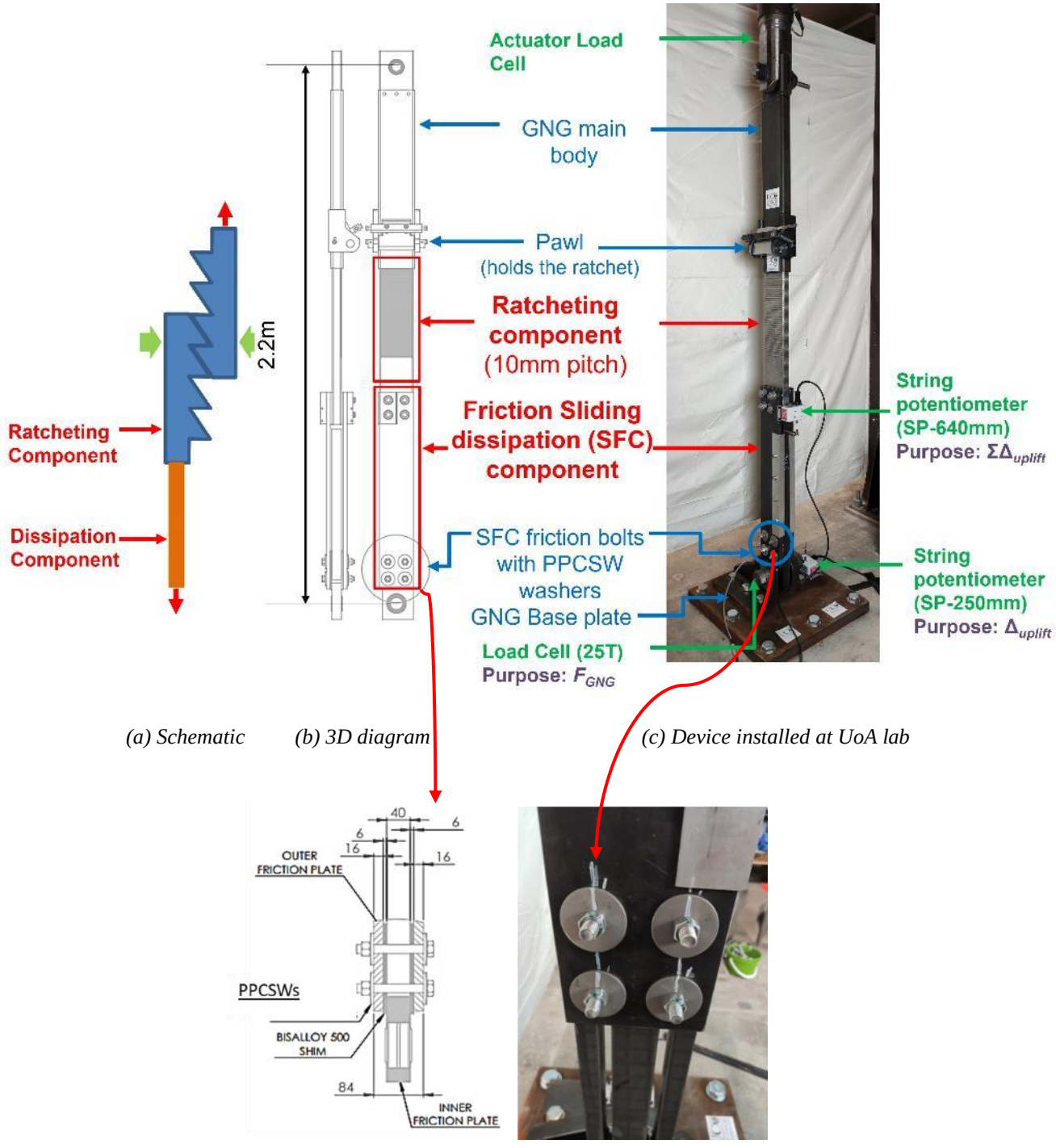

(a) Schematic *(b) 3D diagram* *(c) Device installed at UoA lab*

(d) Friction Sliding connection (SFC) (left) and PPCSWs details (right) where 4 M12 bolts are post-tensioned to achieve 90kN clamping force

Figure 3: Grip and Grab (GNG) device test specimen

3.2 Test plan

The 2.2m long GNG component device was tested on a 500kN MTS load frame in the Structural Testing Laboratory (STL) at University of Auckland (UoA) (**Figure 3**). Thirty-eight tests were conducted in total. The device was subjected to various unipolar cyclic "extension and return to initial displacement" test regimes to represent the expected demands imposed on such a device attached to a rocking frame, where full post-earthquake recentring is required. The device carries tensile force throughout the cyclic extension, absorbs response energy during frictional sliding, then ratchets to its initial position while just acquiring a small amount of compressive force (less than 1kN) to prevent buckling.

The test programme used M12 equivalent grade 8.8 with 110mm and 120mm bolt length and M16 8.8 grade bolt/nut sets with 120mm bolt length. Here, friction bolts and nuts were tested for quality in accordance with standards NZS 3404.1 [19] and AS/NZS 1252.1 [20] and bolt length was chosen to be long enough to grip the two shims, three plates and two washers in addition to the nut thickness. Bolt washers include standard structural washers and the conical spring washers (CSWs) also known as Belleville springs (BeS) are shown in **Figure 3(b-d).** These were used first used by Ramhormozian [21] in friction connections. These CSWs may be partially post tensioned (PPCSWs) to allow a range of clamping forces. Two nominal total clamping forces were applied from the bolt group**.** These were 90 and 200 kN. Frictional components consisted of 6mm thick shims with Brinell hardness of around 500 (Bisalloy500 [22] as well as JFE EHSP (Ever-Hard Steel Plates) plates Grade 500 which are closest equivalent to Bisalloy500 [23] were used, 40mm thick centre friction plates (Grade 500 steel), and 16mm thick outer friction plates were (Grade 350 mild steel). **Figure 3(d)** displays the details of the frictional components. Shims and the centre friction plate were reused for some tests, and their performance was evaluated. The surface for all the frictional components (inner friction plates and shims) were treated to SA2 after machining using shot as the blast medium. Ratcheting device with tooth pitches of 5mm and 10mm. All these test parameters and the basis for their selection are discussed in depth in Rangwani et al. [24].

3.3 Test protocols

The test protocols (TPs) were in the form of displacement histories. A total of nine TPs were used across all the tests. The TPs varied based on constant amplitudes (CAM) of small (i.e., 25mm), medium (i.e., 50mm) and large (i.e., 120mm) peak amplitudes, increasing displacement histories based on ATC-24, irregular displacement histories obtained from structural simulations using ground motion El-Centro 1940 for 5mm and 10mm tooth pitch size. Other parameters considered were load rate, with normal velocity (V) used was 5mm/s and maximum velocity (V_{max}) used was 9mm/s which was less than maximum machine velocity ($V_{max\_machine}$) of 9.45mm/s. The maximum frequency ($f_{max\_machine}$) was 0.05Hz which was less than maximum machine frequency ($f_{max\_machine}$) of 0.15Hz.

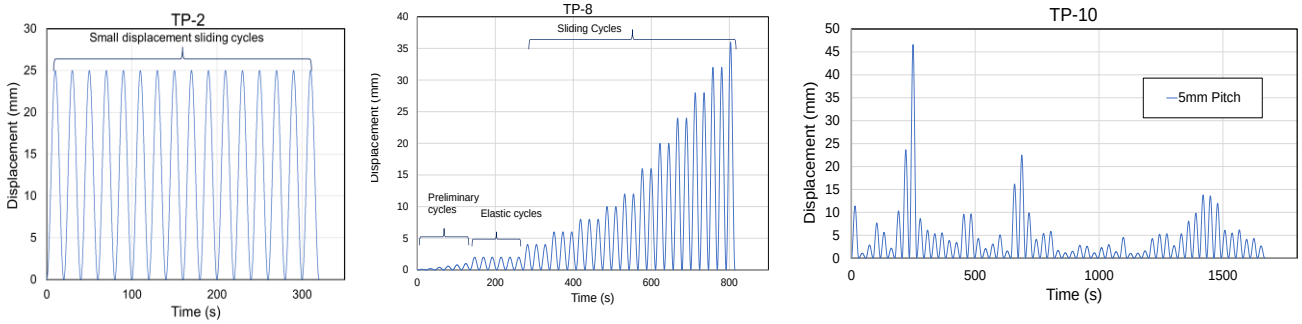

(a) TP-2 Constant amplitude (CAM) of 25mm

(b) TP-8 as per ATC-40

(c) TP-10 obtained from simulations using ground motion EC1940 for the device with 5mm tooth pitch

Figure 4:Test protocols used for the component test.

Additionally, the physical GNG devices were designed and constructed to have 500mm of displacement capacity within the rack and also within the sliding friction connections. Therefore, the maximum device design displacement capacity (CUD_{max_design}) considered was 500mm. The cumulative displacement limit (CUD_{limit}) applied for all the test protocols used for the component tests was 0.9 x CUD_{max_design} i.e., 450mm. The nominal maximum peak-to-peak design uplift displacements were 200mm. Therefore, the maximum device design peak uplift displacement (PUD_{max_design}) considered was 200mm. The peak uplift displacement limit (PUD_{limit}) applied for all the test protocols used for the component tests was 0.9 x PUD_{max_design} i.e.,

180mm.Some of the TPs shown in **Figure 4** below correspond to the respective displacement histories of TP-2 (CAM with small peak displacement (25mm), TP-8 (ATC-24), and TP-10 (obtained from structural simulations using input ground motion EC1940 and using 5mm tooth pitch for the ratchet).

3.4 Instrumentation and control system unit

The University of Auckland MTS load frame used basic test ware as a control system interface. For this test setup, it was simple to incorporate different test protocols, such as an "irregular displacement profile" or "time-history analysis" from structural modelling. The application that was modelled for this testing was placement of the dissipater at the base of a rocking frame. As such, the device was subjected to unipolar motions where the device extended in tension, then returned to the original zero-displacement position, without ever going to a length shorter than the original.

Sensors used were as follows:

- Load pin with 25 tons capacity to record GNG force (F_{GNG}). The load cell is shown at the bottom which connects the GNG device to the pin connection to the baseplate in **Figure 3c**.
- String potentiometer SP-250 (250mm displacement capacity) to record uplift displacement (Δ_{uplift}). This sensor is positioned on the right side of the GNG base plate. The other end of the string is connected to the upper pin connections at the top of the GNG device, as shown on **Figure 3c**. This potentiometer measures the relative displacement between the ram and baseplate, which corresponds to the rocking frame uplift displacement when installed within a structure.
- String potentiometer SP-640 with 640mm displacement capacity to record cumulative displacements ($\Sigma\Delta_{uplift}$). It is clamped on central right corner between the friction plate and ratchet as is highlighted in **Figure 3c**. This potentiometer records the displacement between the lower end of the rack and the inner friction plate, which represents the cumulative inelastic displacement within the sliding friction dissipater.

As stated earlier, Rangwani et al. [24] provides considerable additional information about these sensors and their properties.

4 BEHAVIOUR / PERFORMANCE

Out of a total of 38 tests, this paper only provides the comprehensive test findings for five key tests, due to space limitations. All of these are covered in detail in Rangwani et al. [25].

4.1 Test specifications

Table 1 details the test specifications for 5 tests. The test protocol (TP) used for all these tests was TP-1(corresponds to the initial elastic cycles with peak-to-peak amplitude of upto 2.5mm and total cumulative displacements of 32.5mm) and TP-2 which corresponds to the constant amplitude with small peaks of 25mm upto 16 cycles as shown in **Figure 4(a).** Therefore, maximum cumulative uplift displacement (CUD_{max}) from test protocol (TP-1 and TP-2) was 432.5mm. So, the CUD_{max} applied for these tests was less than the CUD_{limit} <= 0.9 CUD_{max_design} i.e., 450mm. **Table 1** lists the specifications of these tests. The first column in Table 1, Col. (1) listed the test number for each test, Col. (2) listed the design sliding force that was intended to be attained, and Col. (3) listed the diameter and length of the bolts used in each test. The bolt length considered for M12 bolts, where PPCSWs were used, was 120 mm; however, with standard structural washers, the bolt length considered was 110 mm. In addition, the bolt length considered for M16 bolts was 120 mm. Col. (4) describes the GNG device used for Tests 9, 11, and 12 had ratchet teeth with a pitch size of 10mm, while the GNG device used for Tests 23 and 25 had ratchet teeth with a pitch size of 5mm. Cols. (6) and (7) provide details of the specific shim sets with Brinell hardness 500 and specific inner (central) friction plate used for the SFC connection. Cols. 8 to 10 describe proof loading of bolts with a certain bolt tension when implemented with PPCSWs. Rangwani et al. 2023a provides a detailed explanation of the procedures to employ in order to achieve the required bolt tension and the bolt tensioning process. For tests 9 and 26, four M12 bolts were partially post-tensioned with CSWs to achieve a target clamping force of 90kN, for tests 11 and 12, two M16 bolts were partially post-tensioned with CSWs to achieve target clamping force of 90kN and for test 25, four M12 were fully proof loaded to achieve the total target clamping force of 200 kN. The total clamping force (F_D) is the sum of the individual bolt tension forces (*IBT*). In this case, because there were two interfaces and sliding frictional coefficient force (μ) was 0.5, nominal sliding force per bolt was the same as the installed bolt tension. The total sliding force (F_s) is equal to the bolt sliding force times number of bolts. For M12 bolts, total proof load (PL) for 4 bolts was 4 times 50kN which equals to 200kN and for two M16 bolts were 2 times 95kN which equals to 190kN.

Table 1 Test specifications

Test No	F_D (kN)	Bolts diameter & length	Ratchet TP size	PPCSWs (Y/N)	Shims (Grade 500)	IFP	No of bolts PL	%PL	IBT (kN)
(1)	**(2)**	**(3)**	**(4)**	**(5)**	**(6)**	**(7)**	**(8)**	**(9)**	**(10)**
9	90	M12 (120mm)	10	Y	New M12_B1 M12_B2	New M12_2	4	45%	22.5
11	90	M16 (120mm)	10	Y	New M16_B1 M16_B2	New M16_3	4	47%	45
12	90	M16 (120mm)	10	Y	Repeated M16_B1 M16_B2	Repeated M16_3	4	47%	45
23	200	M12 (110mm)	5	N	New M12_5 M12_6	Repeated M12_2	4	100%	50
26	90	M12 (120mm)	5	Y	New M12_9 M12_10	Repeated M12_2	4	45%	22.5

Notations: F_D – Clamping force, BF – Bolt force, PPCSWs – Partially posttensioned conical spring washers, IFP – Inner friction plate, PL – Proof loaded, IBT – Installed tension in each bolt.

4.2 Test results

The response obtained can be presented in the form of Force vs Displacement, Displacement vs time, Force vs Time and Overall system slip vs Time. The forces from the actuator (RAM) were roughly higher by 2.5 kN (i.e., roughly equal to the weight of the device) when compared with the load pin force. The relatively constant difference of around 2.5 kN was due to the RAM carrying extra weight of the device along with the RAM reaction force when the GNG device was pulled in tension. Thus, the load pin forces were considered accurate, and the test results were described based on this force.

Figure 5 displays the test outcomes for Test 9. The findings in **Figure 5(a)** showed a significant change in sliding resistance. Sliding started at 57 kN rather than 90 kN (around 65%), or 35% less than the target design value (F_s = 90 kN). **Figure 5(b)** shows that the displacement time history was slightly different between the ram displacement and the GNG displacement, due to elastic flexibility and take-up on connections. The maximum and average sliding forces were determined from **Figure 5(c)** to be 57 kN and 51 kN, respectively. Inter-cycle sliding degradation was observed from 57 kN to 41 kN (i.e., around 27%) which was not consistent. The strength reduction observed from average sliding resistance (51kN) with respect to actual sliding resistance (90 kN) was around 43%. No change was observed in relative friction bolt rotation during testing. These results are also listed in **Table 2**. As anticipated, the compressive force measured only 0.5 kN, which is only about 1% of the tensile forces induced, as intended by design.

The unreliable performance of the sliding friction connection can potentially be attributed to several factors. The inner friction plates were 40mm thick, which is much thicker than equivalent plate thicknesses for this type of friction connection in prior research. There is the potential for bolt interaction effects from the thicker plate to have influenced performance. Furthermore, the 585mm long slots in the inner friction plates were gas cut, imparting a lot of heat into the plate during the manufacturing process and leading to some bending observed in the plates. This bending may have influenced the contact forces between the shims and the inner friction plate and influenced the sliding friction behavior.

The cumulative sliding displacement (*CSD*) obtained from the Test-9 was 320mm as shown in **Figure 5(d).** This result matched well to maximum cumulative uplift displacement (CUD_{max}) from test protocol (TP-1 and TP-2) (432.5mm) being greater than cumulative sliding displacement (*CSD*).

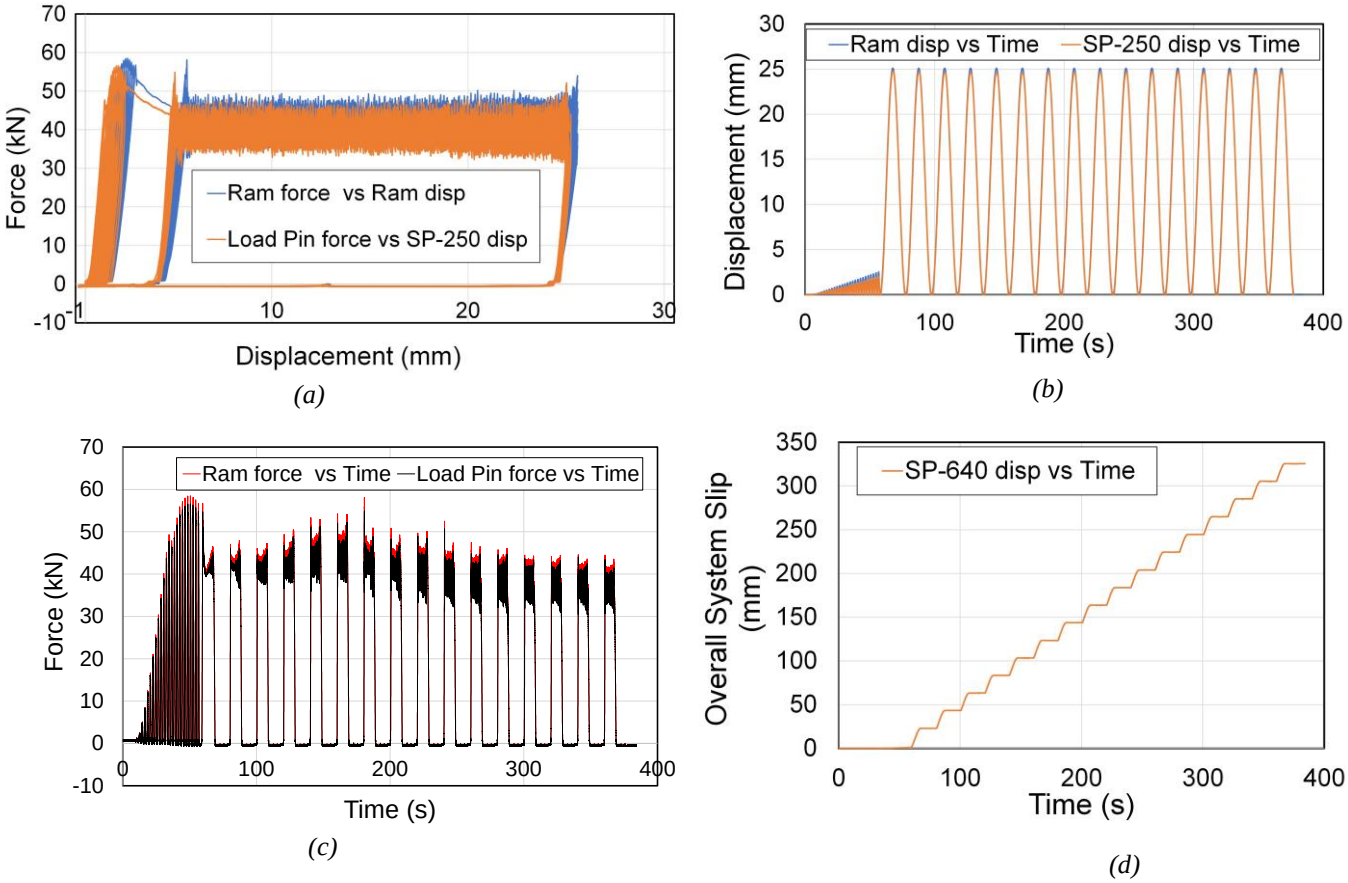

Figure 5: Test 9 Component behaviour when TP-1 (elastic cycles) and TP-2 (CAM at 25mm peak) is applied.

4.3 Friction Sliding forces and Effective Sliding Frictional Coefficient (μ_{eff})

The initial (F_1), maximum (F_{max}) and average (F_{avg}) sliding (tensile) forces were obtained for each test. Variation of the strength of the friction connection was assessed by means of the effective friction coefficient (μ_{eff}) defined as the initial sliding strength (fs) of the connection per bolt (n_{bolts}) (i.e., 2 or 4) and per shear plane (n_{ei}) (i.e., 2 for SFC) divided by the bolt proof load (N_{tf}) (i.e., 95 kN for M16 and 50 kN for M12 with standard washers).

For the current study, the sliding strengths considered were based on initial sliding resistance (F_1) and average sliding resistance (F_{avg}) obtained from test results to derive average effective friction coefficient ($\mu_{eff*avg}$) and initial effective friction coefficient ($\mu_{eff*ini}$).

$$\mu_{eff} = \frac{fs}{n_{bolts} * n_{ei} * N_{tf}} \quad (1)$$

4.4 Comparison of test results.

The test results for Tests 9, 11, 12, 23, and 26 are presented in **Table 2.** Col. (1) listed the test number for each test, Col. (2) listed the design sliding force that needed to be attained, and Cols. (3 to 5) describes the sliding forces obtained for each test at initial cycle (F_1), Inter-cycle maximum sliding force (F_3), sliding force at last cycle (F_4). The maximum (F_{max}) and average (F_{avg}) sliding forces were obtained for all these tests and are listed in Cols. (6) and (7). The average ($\mu_{eff*avg}$) and initial ($\mu_{eff*ini}$) effective coefficient of friction is obtained as per **Equation 1 (Section 4.3)** and is listed for all tests in Cols. (8) and (9). The average tangent stiffnesses (k_{avg}) were obtained for all these tests are shown in Col. (10) and the error difference between them was within 20%. The elastic deformation ranged from 0.71mm to 1.9mm and is listed in Col. (11). For all these experiments, the strength degradation was determined in relation to inter-cycle maximum sliding force and initial sliding force and is listed

in Cols. (12) and (13). Also, the average sliding force (F_{avg}) and actual design sliding forces (F_S) were compared in order to determine the strength degradation, and the results are presented in Col (14). Last but not least, **Table 2**'s Col. 15 lists the maximum compressive forces, which were determined to be much less than 1kN.

Table 2

		Load Pin (tensile force)									***Strength degradation***			***Compressive force***
Test No	F_s	F_1	F_3	F_4	F_{max}	F_{avg}	$\mu_{eff*avg}$	$\mu_{eff*ini}$	k_{avg}	Δ_e	F_4 w.r.t F_3	F_4 w.r.t F_1	F_{avg} w.r.t F_s	F_{c_max}
	kN	*kN*	*kN*	*kN*	*kN*				*kN/m*	*mm*	*%*	*%*	*%*	*kN*
(1)	**(2)**	**(3)**	**(4)**	**(5)**	**(6)**	**(7)**	**(8)**	**(9)**	**(10)**	**(11)**	**(12)**	**(13)**	**(14)**	**(15)**
9	90	57	55	41	57	51	0.28	0.32	72191	0.71	25	27	43	0.46
11	90	80	62	27	80	57	0.31	0.45	71556	0.79	56	66	37	0.43
12	90	98	104	60	104	88	0.49	0.55	86545	1.01	43	39	3	0.45
23	200	118	185	183	185	162	0.4	0.3	85144	1.90	1	54	19	0.51
26	90	50	89	88	89	75	0.42	0.28	71623	1.05	2	77	16	0.42

Notations: F_s – Total Design Sliding Force, F_1 – Initial Sliding Resistance (ISR), F_3 – Intercycle maximum sliding resistance, F_4 – Sliding resistance at last cycle, F_{max} – Maximum Sliding Resistance, F_{avg} – Average Sliding Resistance, $\mu_{eff*avg}$ – SFC frictional coefficient based on F_{avg}, $\mu_{eff*ini}$ – SFC friction coefficient based on initial resistance F_1, k_{avg} – Tangent stiffness, Δ_e – elastic deformation. F_4 *w.r.t* F_3 – Strength Degradation with respect to Intercycle max sliding resistance, F_4 *w.r.t* F_1 – Strength Degradation with respect to initial sliding resistance, and F_{avg} *w.r.t* F_D – Strength reduction with respect to actual sliding resistance, F_{c_max} – Maximum compressive force.

4.4.1 Comparison of test results with varying bolt sizes

Tests 9 and 11 are compared where 4 x M12s and 2 x M16s bolts are partially post-tensioned used to achieve a clamping force of 90 kN with CSWs. New bisalloy shims (Grade 500) and inner friction plates are used. It is observed that the elastic deformation (Δ_e) achieved in both cases is 0.71mm and 0.79mm, respectively, which is within a 10% variation interval. While Tests 9 and 11 both had maximum sliding forces of 57 kN and 80 kN, respectively, their average sliding forces were 51 and 57 kN, respectively. The strength degradation observed with respect to initial sliding resistance for Test 11 (M16 bolts) was higher by 59% as compared to Test 10 when M12 bolts were used. In both of these cases, the maximum compressive force was less than 1 kN. The cumulative sliding displacement (CSD) obtained from both these tests was 320mm. This result matched well to maximum cumulative uplift displacement (CUD_{max}) from test protocol (TP-1 and TP-2) 432.5mm being greater than cumulative sliding displacement (*CSD*).

4.4.2 Reusability of Shims and inner friction plates (IFP)

Tests 11 and 12 are compared where two M16s bolts are partially post-tensioned to achieve the total clamping force of 90 kN with CSWs while the other two bolts were finger tight and snug tight for the respective tests. The reusability of frictional components is what differentiates the two tests. Also, new bolts, new Grade 500 bisalloy shims, and a new inner friction plate (IFP) was used in Test 11. All of these components were cleaned with acetone before being used again in Test 12.

For Test 11, initial sliding frictional resistance obtained was 80 kN instead of 90 kN (i.e., around 89% of design sliding force) and then the strength drops to 27 kN for later cycles i.e., almost 66% strength degradation was observed whereas for Test 12, the maximum sliding frictional resistance obtained was 98 kN from where the sliding initiated (which was higher than design value of 90 kN) and then reduced to 60 kN (i.e., around 67% of design sliding force) i.e., about 39% strength degradation was observed within this test. Also, it can be seen from the findings that for Tests 11 and 12, the average sliding force's strength degradation with respect to the design sliding resistance was 37% and 3%, respectively. In both of these cases, the maximum compressive force was less than 1 kN. The cumulative sliding displacement (CSD) obtained from both these tests was 320mm.

Bisalloy shims (M16_B1 and M16_B2) condition after being used in Test 11 is shown in **Figure 6(a)**, while **Figure 6(b)** depicts the same shims' condition after being used again in Test 12. The images show that shims M16_B1 and M16_B2 were more worn after being used repeatedly for Test 12 than for Test 11.

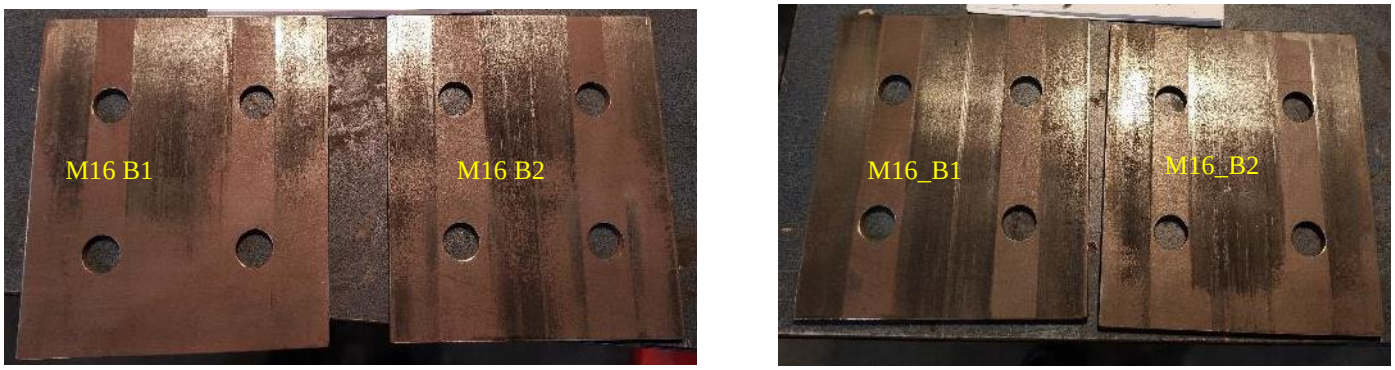

(a) New Bisalloy shims Grade 500 used for Test 11

(b) Bisalloy shims Grade 500 reused for Test 12

Figure 6 Condition of shims after tests 11 and 12

4.4.3 Comparison of test results using GNG ratchets with tooth pitches of 5mm and 10mm.

Tests 9 and 26 use GNG ratchet tooth size of 5mm and 10mm, respectively. For both these tests four M12s bolts are partially post-tensioned to achieve the total clamping force of 90 kN with CSWs and other test conditions are described **in Table 2**. For Test 9, initial sliding frictional resistance obtained was 57 kN instead of 90 kN and then the strength drops to 41 kN for later cycles i.e., almost to 27% strength degradation was observed whereas for Test 26, an initial sliding frictional resistance of 50 kN was obtained from where the sliding initiated and then gradually increased to 89 kN i.e., almost to 77% strength increase was observed. It is observed from the test results in **Table 2**, that maximum and average sliding forces for Test 9 with 10mm tooth pitch size ratchet are lower by 36% and 32% respectively as compared to Test 26 where 5mm tooth pitch size of ratchet was used. Also, it can be seen from the results that for Tests 9, the average sliding force's strength degradation with respect to the design sliding resistance was more by 63% than that for Test 26.

4.4.4 Comparison of test results with and without the use of partially post-tensioned conical spring washers

The test requirements for Tests 23 and 26 are listed in **Table 1,** rows 4 and 5. CSWs were used with four M12 bolts for Test 26 and were partially post-tensioned to achieve the total clamping force of 90 kN. The standard structural washers with four M12 bolts were used for Test 23 and were fully proof loaded to achieve the total clamping force of 200 kN. The ratchet tooth pitch size considered was 5mm. All other specifications for these tests were the same. The inner friction plate was cleaned and used again for both tests, and the shims were new.

For Test 23, initial sliding frictional resistance obtained was 118 kN instead of the target design sliding force of 200 kN, and then the strength increased to 183 kN for later cycles i.e., almost to 54% increase in the strength was observed whereas for Test 26, initial sliding frictional resistance obtained 55 kN from where the sliding initiated and then gradually increased to 89 kN i.e., almost to 77% strength increase was observed. Also, it can be seen from the results that for Tests 23, the average sliding force's strength degradation with respect to the design sliding resistance was more by 16% than that for Test 26.

For both Tests 23 and 26, the maximum compressive force was less than 1 kN (0.42 kN and 0.51 kN respectively). Both of these tests showed cumulative sliding displacements (CSD) of 323mm and 325mm, respectively This result matched well to maximum cumulative uplift displacement (CUD_{max}) from test protocol (TP-1 and TP-2) 432.5mm) being greater than cumulative sliding displacement (CSD).

4.4.5 Sliding Frictional Coefficient (μ_{eff})

It is observed from the results in **Table 2**, the average and initial effective frictional coefficients ($\mu_{eff*avg}$ and $\mu_{eff*ini}$) obtained from the experimental tests (Tests 9, 10, 12, 25) with PPCSWs were 0.38 and 0.4 and the values obtained from test with standard washers (Test 23) were 0.4 and 0.3 respectively. These values are low as compared to the design value (μ_{design} = 0.5).

5 CONCLUSIONS

1. How does the device behave?

The following outcomes were attained by friction GNG's overall performance.

a. The device responded with frictional sliding in tension and ratchet in compression. As a result, there was no presence of any buckling under compression, in contrast to conventional compression-tension dissipators.
b. The compression force was minimum (< 1kN) as expected.
c. Residual compressive forces were essentially eliminated.
d. The ratcheting device performed well, with no degradation in performance or any visible damage.
e. No self-loosening of the friction bolts was observed.
f. Yielding of bolts was prevented.
g. The cumulative inelastic displacement obtained from the testing within the sliding friction dissipater (*CSD* = 320mm) was within 30% of the predicted CUDs (i.e., CUD_{max} = 432.5mm).

2. Can such a GNG frictional device be designed and constructed?

The GNG frictional device was designed with the ratcheting component and the dissipation (frictional) component and is planned to be implemented in full-scale shake-table test of the ROBUST rocking frame building as a low damage design. Seismic response energy is absorbed within the device when it is loaded under tension by sliding in the frictional component. Almost no force is carried when the device is loaded in the compression direction. Therefore, the device does not buckle, but relative displacement occurs in the ratcheting component. The ratcheting during the shortening of the device as the frame base returns to the foundation will allow recentring of the rocking wall. Thus, GNG frictional devices can be designed and constructed for their application in rocking structures in NZ and worldwide.

3. Does the device behave predictably and consistently?

The friction GNG device's ratcheting component performed well overall, operating reliably and showing no degradation or any visible damage. The sliding friction connection was less reliable and the desired forced in friction component wasn't completely achieved. These are covered below:

Frictional Component Behaviour

a. Consistent sliding force was not achieved with and without PPCSWs.
b. Sliding resistance in tension achieved was in the range 20-40% less than the expected target design values, with and without PPCSWs.
c. Average effective sliding coefficient obtained from the tests were approximately 24% lower than the previously published designed values.

Possible reasons for not achieving the expected sliding resistance.

a. Bolt plate interaction (i.e., transfer of bolt force) – the inner friction plates were 40mm thick, which is much thicker than equivalent plate thicknesses in prior tests. There is the potential for bolt interaction effects from the thicker plate to have influenced performance.
b. Alignment and thickness of central frictional plate. As well as having a larger thickness than plates in previous tests, the 585mm long slots in the inner friction plates were gas cut, imparting a lot of heat into the plate during manufacturing and leading to some bending observed in the plates. This bending may have influenced the contact forces between the shims and the inner friction plate and influenced the sliding friction behavior.
c. Bolt tightening sequence. Several bolt tightening sequences can be applied across the clamping bolt group. Further research is needed to ascertain whether the specific bolt tightening sequence influences the frictional performance.

6 OUTCOMES/ADVANTAGES

Component behaviour of friction GNG (supplementary) energy dissipation device will be helpful in design and its application for rocking structures in NZ and worldwide.

7 FUTURE SCOPE

To better understand the causes of the low sliding friction resistance from GNG component tests, a parametric research and experiments on the sliding friction dissipator (SFC) will be carried out, where inner friction plate thickness and bolt tightening sequence will be investigated. The inner friction plates will be machined differently to minimize plate bending and individual washer loadcells will be used to measure bolt axial load during tests.

8 ACKNOWLEDGEMENTS

Financial support for the experimental work from Catalyst Company is gratefully appreciated. Donations of materials is kindly provided by D&H Steel. Many Thanks to UC QuakeCoRE for their support to the first author. Last but certainly not the least, the authors are thankful to the University of Auckland and University of Canterbury laboratory technicians for providing support with the test and fabrication process. Special thanks to UoA technician Mark Byrami for all his help to the primary author during the testing process. The QuakeCoRE paper number is **0797.**

9 REFERENCES

[1] Gultom, R., & Ma, Q.T. (2015). "Biaxial pseudo dynamic tests of a post-tensioned rocking column with externally mounted energy dissipaters." *Proceedings of the 2015 NZSEE Annual Conference*, 429-436. Rotorua, New Zealand. http://hdl.handle.net/2292/26824.

[2] Cook, J., Rodgers G.W. & MacRae, G.A. (2018). "Design and Testing of Ratcheting, Tension-Only Devices for Seismic Energy Dissipation Systems." *Journal of Earthquake Engineering* **24**: 1-22. http://doi.org/10.1080/13632469.2018.1441765

[3] Cook, J., Rodgers, G.W. & MacRae, G.A. (2019). "Assessment of cumulative inelastic displacement demand in energy dissipation systems using the Grip 'n' Grab tension-only mechanism." *2019 Pacific Conference on Earthquake Engineering (PCEE)*, Auckland, 4-6 April 2019.

[4] MacRae, G.A., Clifton, C. (2015). "Research on Seismic Performance of Steel Structures in Seismic Areas." *2015 STESSA Conference* Tongji University, Shanghai.

[5] MacRae, G. A. (2010). "Some Steel Seismic Research Issues," in *Proceedings of the Steel Structures Workshop 2010*, Research Directions for Steel Structures, compiled by MacRae G. A. and Clifton G. C., University of Canterbury.

[6] MacRae, G.A. (2013). "Low Damage Construction – Some System Issues." *2013, 10CUEE*, Tokyo Institute of Technology, Japan, 1-2 March 2013.

[7] Wiebe. L., Sidwell. G., Gledhill. S. (2015). "*Design Guideline for Controlled Rocking Steel Braced Frames*", SCNZ Report 110;2015, prepared by Aurecon New Zealand Limited for SCNZ, New Zealand. https://www.scnz.org/wp-content/uploads/2020/11/P4_A-PRACTIONERS-GUIDE-TO-DESIGN-AND-DELIVERY-OF-CONTROLLED-ROCKING-STEEL-BRACED_Gledhill-min.pdf

[8] Rodgers. G.W., Chase. J.G., MacRae. G.A., Bacht. T., Dhakal. R.P., and Desombre. J. (2010). "Influence of HF2V Damping Devices on The Performance of The SAC3 Building Subjected to The SAC Ground Motion Suites", *9USN-10CCEE*, Toronto, July 25-29

[9] Jones, A.S. (2011). "*Low cost, lightweight buckling restrained braces for low rise buildings."* Master's thesis. Civil and Environmental Engineering. University of Auckland. Auckland. New Zealand

[10] Gunning. M., and Weston. D. (2013). *"Assessment of Design Methodology for Rocking Systems."* ENCN493 Report, Department of Civil and Natural Resources Engineering, University of Canterbury, Christchurch, NZ.

[11] Gledhill, S. (2015). "A Practioners Guide to Design and Delivery of Controlled Rocking Steel Braced Frame Structures." *2015 Steel Innovations Conference* Auckland, New Zealand.

[12] Rangwani, K., MacRae, G.A., Rodgers, G.W., Soleimankhani, H., J. Cook. (2020). "Tension-only device for a steel rocking frame system." *NZSEE Conference*, Wellington, New Zealand, 22-24 April 2020.

[13] Rangwani, K.P., MacRae, G., and Rodgers, G.W. (2023) "Performance of rocking frames with friction tension-only devices." *Early access. Bulletin of the New Zealand Society for Earthquake Engineering*, Vol. 56, No. Y, Month 2023. https://doi.org/10.5459/bnzsee.1583

[14] Rad, A. & MacRae, G.A. (2017). "Dynamically Straightening of Low-Damage Steel Buildings after Earthquake." *Proc., Resilience – the new challenge in earthquake engineering, WCEE16*, Santiago Chile.

[15] Rad, A.A., Hazaveh, N.K., MacRae, G.A., Rodgers, G.W., Ma, Q. (2019) "Structural straightening with tension braces using aftershocks – Shaking table study." *Soil Dynamics and Earthquake Engineering* 123: 399-412, Doi: 10.1016/j.soildyn.2019.05.005.

[16] Livia, E., Yoo, J. and MacRae, G.A. (2019). "Development of a tension-only friction dissipater for rocking wall." *2019 Pacific Conference on Earthquake Engineering, (PCEE)*, Auckland, 4-6 April 2019.

[17] Yan, Z., Ramhormozian, S., Clifton, G.C., Bagheri, H., Rangwani, K., MacRae, G.A., Quenneville, P., Dhakal, R., Xiang, P., Jia, L., & Zhao, X. (2021). "Three-storey Configurable Steel Framed Building Incorporating Friction Based Energy Dissipater: Structural Configuration and Instrumentation." *NZSEE Conference*, 14 - 16 April 2021, University of Canterbury, Christchurch.

[18] MacRae, G.A., Zhao, X., Clifton, C., L-J. Jia, Dhakal, R., Xiang, P., Ramhormozian, S., Rodgers, G. (2020). "The China-NZ ROBUST Friction Building Shaking Table Testing Overview." *WCEE17*, Sendai, Japan.

[19] Standards New Zealand (2007). *"NZS3404: Part 1. Steel Structures Standard, Part 1*". Standards Association of New Zealand, Wellington, NZ. https://www.standards.govt.nz/shop/nzs-3404-parts-1-and-21997

[20] Standards New Zealand. (2016). "*AS/NZS1252: High-strength steel bolts with associated nuts and washers for structural engineering."* in Australia/New Zealand Standard.

[21] Chanchi, J.C., MacRae, G.A., Chase, G., Rodgers, G., and Clifton, C. (2012). "Behaviour of asymmetrical friction connections using different shim materials." *New Zealand Society for Earthquake Engineering Conference.*

[22] Total Steel (1999). "*A complete report to JFE EVERHARD EHSP JFE's Super Abrasion Resistant Steel Plates. Technical Bulletin 2. Total Steel of Australia Pty Ltd."* Google. https://www.totalsteel.com.au/assets/files/technical/jfe-ehsp-tests.pdf

[23] Ramhormozian, S. (2018). *"Enhancement of the Sliding Hinge Joint Connection with Belleville Springs"* in Department of Civil and Environmental Engineering. University of Auckland: Auckland, New Zealand.

[24] Rangwani, K.P., Rodgers, G., and MacRae, G. (2023a) "Frictional GripNGrab Component Tests." *In draft. Journal of Earthquake Engineering*, Vol. XX, No. Y, Month 2023.

[25] Rangwani, K.P., Rodgers, G., and MacRae, G. (2023b) "Frictional predictability of GripNGrab Device." *In draft. Journal of Earthquake Engineering*, Vol. XX, No. Y, Month 2023.